DOE/NASA/2674-79/6
NASA TM-79195

PERFORMANCE CHARACTERISTICS OF A SLAGGING GASIFIER FOR MHD COMBUSTOR SYSTEMS

Kenneth O. Smith
National Aeronautics and Space Administration
Lewis Research Center

June 1979

Prepared for
U.S. DEPARTMENT OF ENERGY
Energy Technology
Magnetohydrodynamics Division

DOE/NASA/2674-79/6
NASA TM-79195

PERFORMANCE CHARACTERISTICS OF A SLAGGING GASIFIER FOR MHD COMBUSTOR SYSTEMS

Kenneth O. Smith
National Aeronautics and Space Administration
Lewis Research Center
Cleveland, Ohio 44135

June 1979

Work performed for
U. S. DEPARTMENT OF ENERGY
Energy Technology
Magnetohydrodynamics Division
Washington, D. C. 20545
Under Interagency Agreement EF-77-A-01-2674

PERFORMANCE CHARACTERISTICS OF A SLAGGING GASIFIER FOR MHD COMBUSTOR SYSTEMS

Kenneth O. Smith
NASA Lewis Research Center
Cleveland, OH 44135

Abstract

The performance of a two-stage, coal combustor concept for MHD systems was investigated analytically. The two-stage MHD combustor comprises an entrained flow, slagging gasifier as the first stage and a gas phase reactor as the second stage. The first stage was modeled by assuming instantaneous coal devolatilization and volatiles combustion and char gasification by CO_2 and H_2O in plug flow. Heterogeneous surface reaction rates were determined from experimental data in the literature. Gasifier heat loss was treated parametrically. Slag effects were not considered. The second-stage combustor was modeled assuming adiabatic instantaneous gas phas reactions. Of primary interest was the dependence of char gasification efficiency on first-stage particle residence time. The influence of first-stage stoichiometry, heat loss, coal moisture, coal size distribution, and degree of coal devolatilization on gasifier performance and second-stage exhaust temperature was determined. Performance predictions indicate that particle residence times on the order of 500 msec would be required to achieve gasification efficiencies in the range of 90 to 95%. The use of a finer coal size distribution significantly reduces the required gasifier residence time for acceptable levels of fuel-use efficiency. Residence time

requirements are also decreased by increased levels of coal devolatilization. Combustor design efforts should maximize devolatilization by minimizing mixing times associated with coal injection.

Introduction

The U.S. Department of Energy is currently directing a program to demonstrate the feasibility of a coal-fired, open-cycle magnetohydrodynamic (MHD) system for electric power generation. An MHD system operating as a topping cycle above a conventional steam cycle has the potential to significantly increase overall system efficiency[1]. One component of the MHD system requiring considerable developmental work is the coal combustor. This report is concerned with the performance characteristics of a particular two-stage combustor concept being considered for use in MHD systems [2,3]. This two-stage combustor is comprised of a slagging gasifier first stage followed by a gas-phase combustor.

The fundamental requirement of any MHD combustor will be to generate a high-temperature exhaust flow. Exit temperatures must be sufficiently high so that seeding of the exhaust flow produces a plasma with an acceptable electrical conductivity. A minimum acceptable exhaust temperature will be on the order of 2800^{o}K. Two-stage combustor concepts are proposed for MHD systems because of the probable need to limit the amount of coal ash exhausted from the combustor. Components downstream of the combustor will dictate permissible levels of ash carryover. The first stage of a two-stage combustor produces a gaseous fuel from coal and serves to separate coal ash or slag from the

fuel gas. The relatively ash-free fuel gas is subsequently burned in the second stage to generate a high-temperature exhaust flow.

The slagging gasifier, two-stage combustor concept requires fuel-rich operation of the first stage. Preheated air and pulverized coal feed rates maintain the first-stage equivalence ratio between 2.0 and 2.5. Air preheat temperatures as high as 1920K may be necessary to achieve the desired second-stage exhaust temperature. The first stage stoichiometry is used to control the gasifier temperature so that the coal ash liquefies but does not vaporize. Most commonly, liquid slag entrained in the gasifier flow is separated from the CO-rich fuel gas by means of a swirling flow pattern in the first stage. The swirl acts to centrifuge slag droplets to the walls. Gravity drives the wall slag layer to a tap for slag removal from the combustor. The fuel gas produced in the gasifier is burned in the second-stage combustor with sufficient preheated air to bring the overall system equivalence ratio close to unity.

Although the slagging gasifier, two-stage combustor is an attractive concept for MHD systems because of its slag separation capabilities, its viability will be determined by the maximum attainable exhaust temperature. The first-stage heat loss will be a dominant influence on the exhaust temperature. Heterogeneous reactions in the first stage will be relatively slow because of low oxygen concentrations, and, consequently, long particle residence times will be necessary to insure efficient fuel utilization. However, long residence times are associated with large combustors and large wall

heat losses. The success of the two-stage concept depends upon providing sufficient first-stage residence time for efficient fuel utilization and slag separation while maintaining tolerable heat losses.

To aid in the development and assessment of slagging gasifier two-stage combustor designs, the present study was conducted primarily to examine the dependence of first-stage coal gasification efficiency on particle residence time. The influence of gasifier performance on the second-stage exhaust temperature was also considered. The goal of this study was not to develop or assess a specific combustor design, but to determine the sensitivity of gasifier performance to system operating parameters. A plug-flow reactor model incorporating a simple coal particle gasification model was used for the first stage. The combustor heat loss was treated parametrically. Slag effects were neglected. Experimental data from the literature were used to deduce surface reaction rate expressions for char reactions with CO_2 and H_2O at elevated temperatures[4,5]. The effects of coal moisture, coal size distribution, heat loss, equivalence ratio, and degree of coal devolatilization on gasifier performance were investigated to determine where significant gain in performance can be achieved.

Theory

Nomenclature

C_p	specific heat
D	diffusion coefficient
D_o	diffusion coefficient at T_o and P_o
d	characteristic particle diameter

H^o	enthalpy of formation at T_r
h_T	total enthalpy of inlet coal and air mixture
K(T)	equilibrium constant
$\mathcal{M}$	molecular weight
n_p	number of particles
Nu	Nusselt number
P_o	reference pressure for diffusion coefficient D_o
Pr	Prandtl number
q_j	char mass gasified in particle size range j in time t
q"	specific char gasification rate (per unit surface area)
q_T	total char mass gasified in time t
Re	Reynolds number
T	gas temperature
$\bar{T}$	characteristic gas temperature in particle boundary layer
Δt	time step magnitude
T_o	reference temperature for diffusion coefficient D_o
T_r	reference temperature for enthalpy
T_s	particle surface temperature
X^e	equilibrium gas phase wide fraction
X^o	nonequilibrium gas phase wide fraction
Y	gas phase mass fraction
α	surface reaction rate
η	char gasification efficiency
ξ	devolatilization parameter (eqn. 1)
$\bar{\rho}$	characteristic gas density in particle boundary layer

τ first-stage combustor particle residence times

ϕ_1 first-stage fuel equivalence ratio

Ψ, Ψ' equilibrium conversion parameters (eqns. 8 and 10)

subscripts

i species index

j particle size range index

First Stage Combustor Model

The first-stage gasifier was modeled as a plug flow reactor. The gasifier model assumed:

1) Complete mixing of the inlet air and coal at the gasifier inlet plane.

2) Instantaneous coal devolatilization and volatiles combustion.

3) Heterogeneous char gasification subsequent to volatiles combustion.

4) Local gas phase equilibrium throughout the gasifier.

5) No effects of coal slag on the first-stage performance.

i) Devolatilization

Coal devolatilization was assumed to produce O_2, H_2, N_2, and C through thermally neutral reactions. The degree of coal devolatilization was specified by defining a devolatilization parameter :

$$\xi = \frac{\text{mass of DAF coal volatiles}}{\text{mass of DAF proximate analysis volatiles}} \qquad (1)$$

Experimental studies have established that rapid heating of coal particles ($\sim 10^4$ ^oK/sec) produces more volatiles than are indicated

by the coal proximate analysis[6]. Values of this devolatilization parameter as large as 1.5 may be attainable at the conditions of the first-stage gasifier[7].

Characteristic coal devolatilization times associated with rapid particle heating are on the order of 10 to 20 msec[7]. Since char gasification times will be shown to be at least an order of magnitude larger, instantaneous devolatilization was assumed. The specified inlet coal size distribution was unchanged by the devolatilization process. Solid-phase mass loss during devolatilization resulted only in a decrease in the coal density.

The assumption of instantaneous devolatilization and volatiles combustion allowed gas phase properties subsequent to these processes to be determined by equilibrium calculations. Specified values of the gasifier equivalence ratio and the devolatilization parameter determined the reactants associated with volatiles combustion. First-stage equivalence ratio established the coal to air mass ratio. The devolatilization parameter determined the mass of coal converted to volatiles. Volatiles were assumed to be the H_2, O_2, and N_2 content of the coal with C comprising the remaining volatiles mass. Coal moisture was also released during devolatilization. The products of volatiles combustion were determined using the computer program described in ref. 8.

ii) Reactor Model

Computer calculations of char gasification were conducted using the gas phase properties subsequent to volatiles combustion as initial conditions. The initial mass of char to be gasified was that fraction of the inlet coal still in the solid phase following devolatilization. Char gasification was modeled as if occurring in a plug flow reactor. Combustor heat losses were not modeled directly. Rather, heat loss effects on combustor performance were included by assigning an artificial char enthalpy consistent with the specified heat loss and the coal heating value.

The plug flow reactor program calculated the level of char gasification as a function of particle residence time in the first-stage gasifer. A Euler computational technique was adopted. Char gasification rates calculated at a time t, for each of the particle size ranges employed, were assumed constant for a small time increment. This time increment, Δt, varied from 1 msec early in the gasification process, when conversion rates were high to 25 msec when gasification had slowed significantly. The specific particle gasification model used to determine gasification rates will be described subsequently.

Char gasification was assumed to proceed through two reactions:

$$C + CO_2 \rightarrow 2CO$$

$$C + H_2O \rightarrow CO + H_2$$

The char gasified in the j^{th} particle size range during the time interval Δt was:

$$q_j = np_j \, \pi \, d_j^2 \, q_j'' \, \Delta t \qquad (4)$$

The total char gasified in Δt was:

$$q_T = \sum_j q_j \qquad (5)$$

At the end of each time step the following sequence of calculations was performed:

1) The mass of char in each size range was adjusted to reflect the mass loss by gasification.

2) A new characteristic particle diameter was calculated for each size range. Gasification was assumed to proceed at constant char density and decreasing particle size.

3) Gas phase species concentrations were adjusted to reflect the generation of CO and H_2 and the depletion of CO_2 and H_2O through gasification.

4) The new gas phase mixture was assumed to equilibrate through the water-gas reaction:

$$CO + H_2O \rightleftharpoons CO_2 + H_2 \qquad (6)$$

A new gas temperature was determined simultaneously with the gas phase equilibrium species concentrations.

An iterative technique was adopted to determine the gas temperature and equilibrium composition for each time step. This technique found simultaneous solutions for the equilibrium and energy conservation relationships through the following series of calculations:

1) Gas phase equilibrium concentrations were calculated assuming a gas temperature equal to the temperature at the end of the previous time step. Equilibrium calculations were conducted by assuming the gas phase equilibrated by the forward reaction:
$H_2O + CO \rightarrow CO_2 + H_2$. By defining a degree of conversion parameter Ψ

$$\Psi = \frac{X^o_{H_2O} - X^e_{H_2O}}{X^o_{H_2O}} \tag{7}$$

the equilibrium relation was written:

$$\frac{X^e_{CO_2} X^e_{H_2}}{X^e_{H_2O} X^e_{CO}} = \frac{(X^o_{CO_2} + \Psi X^o_{H_2O})(X^o_{H_2} + \Psi X^o_{H_2O})}{(X^o_{H_2O} - \Psi^o X_{H_2O})\, X^o_{CO} - \Psi X^o_{H_2O})} \tag{8}$$

This was arranged in a quadratic form and easily solved for Ψ. If a root existed for $0 \leq \Psi \leq 1$ then the assumed reaction direction was correct and equilibrium species concentrations could be determined. If no such value for Ψ existed, the reverse reaction occurred. A similar method of solution was followed by using a parameter Ψ':

$$\Psi' = \frac{X^o_{H_2} - X^e_{H_2}}{X^o_{H_2}} \tag{9}$$

A root of the equilibrium relation then existed for $0 \leq \Psi' \leq 1$. Equilibrium constants for the water-gas reaction were obtained from ref. 9.

2) With the calculated species concentrations, a gas temperature was calculated from the energy relation:

$$T = \frac{h_T - \sum Y_i h_i^o}{\sum_1 Y_i cp_i} \qquad (10)$$

Constant species specific heats were assumed.

3) If the assumed and calculated temperatures differed by less than 5^oK, the two relations were assumed satisfied. For larger differences, the sequence was repeated using the calculated gas temperature as the new initial assumed gas temperature.

Since changes in the species concentrations and temperature were small for the small time steps used, typically only a few iterations were necessary to satisfy the two constraints.

iii) Char Gasification Model

Instantaneous char gasification rates were calculated for each time step using a quasi-steady particle gasification model based on the combustion model discussed by Field et al[5]. A fundamental assumption of the gasification model was that the combustion of a large mass of volatiles in the fuel-rich first stage acted to deplete the oxygen available for heterogeneous reactions. Therefore, the only heterogeneous reactions considered significant were char reactions with H_2O and CO_2. The combustion reaction:

$$2C + O_2 \rightarrow 2CO \qquad (11)$$

was neglected. A comparison of the overall char removal rates of these three reactions for species concentrations and temperatures typical of

the slagging gasifier tended to support this assumption. The combined gasification rate due to CO_2 and H_2O reactions was approximately four times greater than the char combustion rate by O_2. The exclusion of the char/O_2 reaction as a char removal mechanism was deemed consistent with the level of modeling employed.

The particle gasification model assumes that spherical particles react at their surface with CO_2 and H_2O. Reaction attributable to the porous char structure is neglected. Therefore, particles gasify with a decreasing diameter and constant density. The overall particle gasification rate due to a single gas phase reactant can be written as:

$$q''_j = \frac{\left(\frac{12}{M_i}\right) \bar{\rho}\, Y_i}{\frac{d_j}{D_i N_u} + \frac{1}{\left(\frac{\bar{T}}{T_s}\right) \alpha_i}} \qquad (12)$$

$\bar{\rho}$ and $\bar{T}$ are commonly taken as average values in the particle boundary layer. For the gasification calculations in this study, the gas phase and particle surface temperatures were assumed equal. In addition, no relative velocity between the particle and gas phase was assumed to exist, and, therefore, $Nu = 2^{6}$. The terms $d_j/2D_i$ and $1/\alpha_i$ represent, respectively, diffusion and surface reaction resistance terms to particle gasification. As $\alpha_i \to \infty$; $d_j/2D_i$ determines the overall reaction rate. Conversely, when $\alpha_i << 2D_i/d_j$, the gasification is surface-reaction controlled.

Instantaneous char gasification rates for the char/CO_2 and char/H_2O reactions were calculated using the particle gasification model described above. The total char gasified in a single time step was taken as the sum of the char masses gasified through the two reaction mechanisms which were assumed independent. This simplification neglects the coupling between the diffusion rates of the two reactants to the particle surface. In addition, it does not address the possibility of altered reaction mechanisms or surface reaction rates due to the presence of two reactants at the particle surface. With regard to this latter consideration, only limited data are available regarding CO_2 and H_2O reactions with carbon at the elevated temperatures characteristic of MHD combustors. Apparently even less work has dealt with the combined effects of the reactants. With regard to the decoupled reactant diffusion rates assumed for this study, subsequent calculations indicate that the assumption is consistent with the overall technical level of the modeling effort. As will be shown, char gasification at the conditions considered is very nearly a surface-reaction controlled process. Reactant diffusion rates are sufficiently rapid so as to represent only a minor resistance to gasification. Any variation in the reactant diffusion rate resulting from a more realistic treatment of the diffusion process should have only minor effects on the calculated char gasification rate.

Second Stage Combustor Model

The second-stage combustor is a high temperature, gas phase reactor. Rapid reaction rates at these high temperatures suggest that second-stage processes will be mixing-limited. However, characteristic mixing times should be small relative to first-stage particle residence times. Therefore, second-stage processes were assumed to be instantaneous and adiabatic. Equilibrium calculations were conducted to predict the second-stage combustor performance[8]. Combustor exhaust temperatures and mass flow rates were calculated assuming sufficient preheated air was injected in the second stage to burn the first-stage exhaust at stoichiometric conditions. No char or slag particle carryover from the first stage was considered in the second-stage combustor calculations.

Surface Reaction Rate Data

There is a limited amount of experimental data in the literature concerning carbon gasification reactions at elevated temperatures. For this study, overall reaction rate data presented in refs. 4 and 5 were used to determine surface reaction rate expressions for the reactions of char with CO_2 and H_2O. Overall reaction rates were determined in refs. 4 and 5 by examining the rate of weight loss of inductively heated carbon spheres as a function of gas phase reactant concentration and particle surface temperature. Measurements were conducted in a forced convected configuration using gas phase reactants at low temperature and atmospheric pressure.

Surface reaction rates were calculated using eq. 12 to model the gasification process. q''_v, Y_i, d_j, and T_s were available directly as experimental data from refs. 4 and 5. $\bar{T}$ was taken as the average particle boundary layer temperature. $\bar{\rho}$ was calculated using $\bar{T}$. Nu was calculated from[6]:

$$Nu = 2 + 0.69\ Pr^{1/3}\ Re^{1/2} \qquad (13)$$

Initially, diffusion coefficients were calculated from the expressions[6]:

$$D_{CO_2} = Do_{CO_2}\ (T/To)^{1.75}\ (Po/P) \text{ and} \qquad (14)$$

$$D_{H_2O} = Do_{H_2O}\ (T/To)^{1.75}\ (Po/P \qquad (15)$$

with $Do_{CO_2} = 0.154$ and $Do_{H_2O} = 0.253$ when To and Po are 300^0K and $1x10^5$ Pa, respectively. These expressions were employed for the plug flow gasifier calculations. However, their use to determine surface reaction rates resulted in a physically meaningless situation. Diffusion coefficients were too low to predict carbon gasification rates comparable to the measured rates even for diffusion-controlled gasification (infinite surface reaction rate). Therefore, an alternate means of establishing the values of Do_{CO_2} and Do_{H_2O} was adopted. This alternate method assumed that the experimental values of q''_j measured at the highest temperatures (3200K) resulted from diffusion-controlled gasification, as suggested by the authors. Therefore,

$$D_{o_i} = q''_j \left(\frac{M_i}{12}\right) \left(\frac{d_j}{\bar{\rho}\ Y_i N_i}\right) \left(\frac{T_o}{\bar{T}}\right)^{1.75} \qquad (16)$$

Values of Do_{CO_2} and Do_{H_2O} calculated in this manner were, respectively, 40% and 90% larger than the values presented in ref. 6. This discrepancy in diffusion coefficients may be attributable at least partially to the simplified treatment of boundary layer mass transfer in the gasification model. For the experimental conditions of a forced convection process with large temperature variations through the boundary layer (T as large as 2900K), the difficulty in establishing characteristic boundary layer properties is considerable. The values of Do_{CO_2} and Do_{H_2O} calculated from the experimental results represent effective values which, perhaps, should not be expected to have values very similar to true diffusion coefficients. For the situation where gasification occurs with insignificant convective effects and no boundary layer temperature gradient, the use of established diffusion coefficient data was appropriate.

The surface reaction rates of char with H_2O and CO_2 determined from refs. 4 and 5 are shown in fig. 1. The points presented do not necessarily represent experimental data points but points taken from smooth curves drawn by the authors through their data. Surface reaction expressions developed from fig. 1 are:

C/CO_2 $\quad \alpha = 37 (cm/s)$ $\qquad 2460 \geq T_s \geq 1673^0K$ $\qquad (17)$

$\alpha = 2.51 \times 10^9 \exp \frac{-44317}{T_s}$ $\qquad 3270 \geq T_s \geq 2460^0K$ $\qquad (18)$

C/H_2O $\quad \alpha = 4905 \exp \frac{-8215}{T_s}$ $\qquad 2645 \geq T_s \geq 1673^0K$ $\qquad (19)$

$= 3.70 \times 10^{12} \exp \frac{-62\,306}{T_s}$ $\qquad 3070 \geq T_s \geq 2645^0K$ $\qquad (20)$

It should be stressed that these expressions were developed from a limited base of experimental data. Their general validity has not been assessed. As it is shown that char gasification is essentially surface reaction controlled, the importance of reliable high temperature gasification data for gasifier performance predictions is clear.

Combustor Operating Parameters

The following operating conditions were considered in determining the two-stage combustor performance:

1. Inlet air preheat temperature: 1922K
2. Inlet air humidity: 0%
3. Combustor pressure: 6×10^5 Pa
4. First stage equivalence ratio: 2.50, 2.25
5. Second stage equivalence ratio: 1.0
6. First stage heat loss: 0, 5, 10% of coal HHV
7. Second stage heat loss: 0%
8. Coal type: Montana Rosebud

   $C(H_2)_{0.401}\ (O_2)_{0.081}\ (N_2)_{0.014}$

   Heating value = 7035 cal/gm
9. Coal moisture: 5, 10, 15% of coal mass
10. Level of devolatilization ( ): 1.50, 1.25
11. Coal size distribution: 70% minus 200 mesh, seven particle size ranges
    100% minus 200 mesh, four particle size ranges

Mass distributions are presented in Table 1.

Results

i) Base Case Calculations

Typical gasifier temperature and species concentrations are presented in Fig. 2 as functions of the char particle residence times, . These data correspond to a base case from which parametric variations were made. This base case of 10% heat loss and 10% moisture (with ϕ_1 = 2.5, ξ = 1.5, and 70%-200 mesh coal) represents a reasonable estimate of gasifier operating parameters. It should be noted that a coal moisture content of 5% is commonly specified for Montana Rosebud coal for MHD systems[10]. However, for the calculations presented, no inlet air moisture was specified. Therefore, the 10% moisture level represents the combined moisture content of the coal and air. Since for the fuel-rich gasifier conditions the coal and air moisture contents can be comparable, the 10% moisture level may be viewed as representative of an actual coal moisture of 5% and an equal mass of inlet air moisture.

As a consequence of the instantaneous volatiles generation and combustion, the gasifier temperature and species concentrations undergo step changes in magnitude at zero time. This is illustrated in fig. 2 where the inlet gas temperature and carbon mole fraction are shown on the ordinates. A high level of devolatilization reduces the mass of char that must react heterogeneously. For the base case conditions, approximately 1/3 of the coal carbon content remains as a solid following devolatilization.

Subsequent to volatiles combustion, the endothermic gasification reactions generate a CO-rich fuel gas while decreasing the gas temperature, CO_2, and H_2O levels. The char reaction with H_2O is responsible for more char removal than the char/CO_2 reaction because of its higher reaction rate. Decreases in temperature and reactant concentrations with time act to decrease the overall gasification rate. In addition, gasification proceeds more slowly as time increases because of the depletion of the smaller coal particle population. The small particles provide a large surface area for reaction. After approximately 800 msec gasification is extremely slow. Carbon utilization efficiencies near 100% may not be attainable in the gasifier for reasonable particle residence times. Even for a residence time of 1 second, the gasification efficiency is only 96%. Clearly, as residence time increases, so too will the combustor heat loss. A successful slagging gasifier design must optimize the tradeoff between combustor heat loss and gasification efficiency.

As discussed previously, the gasification rate of a char particle is determined by both surface reaction rates and reactant diffusion rates. Calculations for the base case conditions were conducted to determine the importance of these two mechanisms. Figure 3 presents carbon gasification histories for the cases of diffusion-controlled reaction (infinite surface reaction rates) and surface-reaction-controlled gasification (infinite diffusion rates). Also presented is the base case gasifier performance for finite diffusion and surface reaction rates. Clearly, the diffusion-controlled case represents the

most rapid gasification attainable for the specified operating conditions. Gasification is considerably slower under surface-reaction control. A comparision of the base case gasifier performance and the reaction-controlled case indicates that gasification rates are largely determined by the slow surface reactions. Reactant diffusion rates are relatively fast. The success of efforts to accurately predict gasifier performance will be strongly dependent on the accuracy of available kinetic data at elevated temperatures and pressures.

ii) Influence of First-Stage Equivalence Ratio and Degree of Devolatilization

The influence of first-stage equivalence ratio and degree of coal devolatilization on char gasification is presented in fig. 4. A decrease in equivalence ratio from 2.50 to 2.25 produces higher gasifier temperature because of a higher O_2 content during volatiles combustion. The volatiles burn at a more nearly stoichiometric condition. Somewhat more rapid gasification relative to the base case is indicated by the model at the leaner condition. Actual char removal rates would be expected to be even larger than predicted since no char removal by O_2 was considered. Although the more rapid char removal at decreased equivalence ratio suggests that a smaller gasifier could be used, any associated heat loss savings would tend to be diminished by the higher gas temperatures. In addition, the higher temperatures are associated with a larger potential for slag vaporization within the gasifer. Adopting the temperature of 2250K as the level below which vaporization is negligible, the decrease in equivalence ratio increases

by 50% the time during which slag droplets might undergo vaporization. Of course, realistic gasifier designs act to minimize slag exposure to high gas temperatures by incorporating a mechanism to drive slag droplets to the cooled combustor walls.

Although the influence of small changes in equivalence ratio or gasification rates may be relatively small. Figure 4 demonstrates the significant influence of the level of devolatilization. A decrease in the devolatilization parameter from 1.50 to 1.25 results in a significant decrease in char gasification efficiency for reasonable residence times. While instantaneous gasification rates are not markedly changed by a decrease in the devolatilization parameter to 1.25, the mass of char remaining following devolatilization increases significantly. The highest levels of devolatilization are associated with the most rapid coal particle heating. Therefore, the initial mixing of the coal and preheated air represents a critical process in gasifier performance. Coal injection systems should be optimized to minimize mixing times and thus maximize coal particle heating.

iii) Effect of First-Stage Residence Time on Second-Stage Combustor Performance

Although the fuel-use efficiency of the first-stage gasifier directly impacts the MHD system efficiency, the combustion system parameter of overwhelming importance to system performance is the second-stage exhaust temperature. Figure 5 presents the attainable exhaust temperature as a function of first-stage residence time for the base case conditions. Exhaust temperature was calculated assuming

stoichiometric combustion of the gasifier exhaust flow. Unreacted char in the gasifier is assumed lost through the first-stage slag tap.

Figure 5 demonstrates that larger values of residence time are associated with higher final temperatures because of higher coal conversion levels. It should be noted, of course, that heat loss is specified parametrically in figure 5. In reality, for a specific combustor design, the assumed heat loss is correct for only one value of residence time. However, figure 5 does indicate that little benefit in terms of final temperature is achieved for carbon efficiencies greater than 90 to 95% (τ from 300 to 800 msec). This would be illustrated more dramatically in figure 5 if heat loss was permitted to increase with residence time.

A combustor performance parameter of second-order effect on system performance is the second-stage combustor mass flow rate. Figure 5 demonstrates the gain in second-stage mass flow accompanying increases in first-stage residence time. Clearly, higher levels of gasification permit a larger total flow. Beyond approximately 500 msec, however, this increase in mass flow becomes less significant.

iv) Effect of Combustor Heat Loss and Coal Moisture

The influences of combustor heat loss and coal moisture level on gasifier performance is indicated in figures 6 and 7. While heat loss affects the gasifier temperature significantly, little effect on the fraction of coal gasified is observed. Moisture content influences gasifier performance in two opposing ways. On one hand, increased moisture acts as a diluent and, therefore, lowers temperatures. Conversely, the increase in moisture represents a reactant concentration increase which augments char gasification.

Figure 8 presents the effects of coal moisture level and combustor heat loss on second-stage exhaust temperature. Although exhaust temperatures were calculated assuming a gasifier residence time of 1 sec, the small variations in gasifier performance beyond 500 msec suggest that figure 8 is representative for τ > 500 msec. Obviously, increased heat loss is detrimental to combustor performance. Apparently, the drop in gasifier temperature associated with increased moisture is too large to be compensated for by the increased char conversion efficiency. Therefore, increased moisture acts to decrease exhaust temperature.

It should be stressed that the exhaust temperature predictions presented in figure 8 are higher than temperatures that would be attained in actual operation. Slag vaporization, slag rejection, and seed vaporization would all act to lower the exhaust temperature. In addition, the assumed air preheat temperature (1920K) represents an optimistic figure. A more realistic preheat temperature could be as much as 150K lower if the air preheaters are constrained to state-of-the-art capabilities. With a minimum acceptable exhaust temperature on the order of 2820K, it is evident that the viability of this two-stage combustor concept will be dependent largely on the development of a low heat loss gasifier.

v) Effect of Coal Size Distribution

The previous gasifier performance characteristics were investigated assuming a standard pulverized coal size distribution of 70% minus 200 mesh. To determine the advantage if gasifier performance associated

with a finer coal grind, calculations were done for a 100% minus 200 mesh distribution where particle diameters were all smaller than about 80 m. Figure 9 illustrates that the finer coal grind allows a specified level of char gasification to be attained in significantly reduced residence times. The time required to achieve a fuel utilization of 95% is reduced from 800 msec to approximately 450 msec. This improvement in gasifier performance with the finer coal distribution is associated with an increase in the surface area available for reaction. Large particles that require long times to gasify have been excluded from the feedstock. At large residence times, these larger particles represent the majority of the remaining char. This is illustrated in Figures 10a and b. These figures show the changes in the two coal size distributions with gasifier residence time. The persistence of larger particles is evident. Conceptually, increasingly finer coal size distributions result in shorter required residence times. However, from a practical point of view, finer coal grinds are more difficult to handle. In addition, more auxiliary power is required to pulverize coal more finely. Thus, the coal size distribution used can only be determined by overall system considerations.

Figure 9 indicates that a significant improvement in gasifier performance is achieved with a finer coal grind. This advantage results solely from the shorter reaction time of smaller particles. However, an additional factor not reflected in figure 9 could act to further increase the advantage of a finer coal grind. Since the level of coal devolatilization is dependent on the particle heating rate, a finer coal grind may produce a larger mass of volatiles and reduce the

mass of char that must be gasified heterogeneously. Gasifier residence time requirements could be reduced. This effect has not been considered in this study.

Summary and Conclusions

The char gasification calculations of this study are summarized in figure 11. Required first-stage gasifier particle residence time is presented as a function of fuel-use efficiency (η), gasifier heat loss, and coal moisture level. At low levels of conversion efficiency, ($\eta < 90\%$), the required residence time is dependent primarily on η, assuming a fixed coal size distribution and devolatilization level. At higher levels of conversion efficiency, moisture level effects are more significant. Increased moisture acts to decrease particle residence time requirements. However, potential heat loss savings associated with smaller residence times are probably offset by exhaust gas temperature decreases with increased moisture. The added moisture acts as a diluent. In general, gasifier heat loss effects on residence time are relatively small. Of course, heat loss remains the parameter of overwhelming importance in attempting to maximize exhaust temperatures. Figure 11 also demonstrates that significant reductions in gasifier residence time can be achieved by using a finer coal size distribution. In addition, the benefits associated with maximizing coal devolatilization are indicated in this figure.

The results of this study indicate that:

1. First-stage gasifier coal conversion efficiencies will vary from 90 to 95% in the range of input parameters in this study are used.
2. Gasifier particle residence times will have to be on the order of 500 msec to achieve the above efficiencies.
3. There is little conversion efficiency gain for residence times larger than 500 msec because of extremely low gasification rates. Increased heat losses with larger residence times will offset any performance gain.
4. The employed coal size distribution should be as fine as practicable. Overall system considerations, such as tradeoffs between gasifier efficiency and coal handling and auxiliary power requirements will determine the actual size distribution used.
5. Gasifier designs should optimize injector configurations to maximize devolatilization. This would be accomplished by maximizing particle heating rates.
6. The gasifier should be operated as close to stoichiometric as possible while still maintaining slag vaporization at acceptable levels.
7. The accuracy of gasifier performance predictions is largely dependent on the accuracy of surface reaction rate data. A reliable data base for char/CO_2 and char/H_2O reactions at high temperatures and pressures does not exist.

Appendix A - Char Gasification Calculations

Char gasification calculations were conducted for a base case condition defined as:

10% heat loss

10% coal moisture

$\phi_1 = 2.50$

$\xi = 1.50$

1922°K air preheat

The reactants in the gasifier prior to devolatilization can be represented as:

$$2.5k\left\{2.236C + \left[\begin{array}{l} 2.519\ C \\ 0.067\ N_2 + 0.464\ H_2O \\ 0.388\ O_2 \\ 1.905\ H_2 \end{array}\right]\right\} + 25.33\left\{0.21O_2 + 0.79N_2\right\}$$

Devolatilization and volatiles combustion were modeled by assuming the coal components in the square brackets reacted instantaneously with the preheated air. The remaining coal carbon content remained unreactive. Equilibrium calculations gave the relative mole fractions of the volatiles combustion products as well as the mixture temperature. Minor products were neglected and the N_2 mole fraction was adjusted to insure that the sum of the gas phase species mole fractions equalled unity. These relative mole fractions and a carbon balance were then used to establish the number of moles of gas phase constituents following volatiles combustion. The absolute species mole fractions can then be calculated by including the unreacted solid char. These data represent the initial conditions for the char gasification process.

A listing of the computer program used for char gasification calculations is presented below. Typical portions of the program output are included to illustrate the presentation of the initial conditions and gasification characteristics at a specific particle residence time.

Data statements are used to input the following information:

$c_p(i)$ - specific heat of species i (cal/gm^{o}K)

$h_o(i)$ - species i enthalpy of formation at 298^{o}K (cal/gm)

MW(i) - species i molecular weight (gm/mole)

WTPCT (i) - mass fraction of char in particle size range i

d(i) - characteristic particle diameter for particle size range i (cm)

The char enthalpy of formation, $_o(6)$, was adjusted to reflect specified levels of gasifier heat loss as a percentage of the coal heating value.

Additional input data must be provided on computer cards:

P - gasifier pressure (dynes/cm^2)

RHOP - char density (gm/cm^3)

NTOT - total number of moles of all species following volatiles combustion

MC - mass of unreacted char following volatiles combustion (gms)

T - gas temperature following volatiles combustion (^{o}K)

X - mole fractions of species subsequent to volatiles combustion

XP - relative mole fractions of gas phase species following volatiles combustion

NTSTEP - number of time steps performed by program

NESTEP - maximum number of iterations performed to establish equilibrium concentrations for each time step

For the current calculations, NESTEP was set at 10. Ten iterations were never required to establish equilibrium conditions for any time step.

The initial gasifier conditions specified are presented in the first five lines of the program output. Following these data are:

Particle number distribution - number of char particles in each size range

Carbon mass distribution - mass of char in each size range

Average molecular weight of mixture (gm/mole)

Initial enthalpy of mixture (cal/gm)

For each time step the following data are presented:

Elapsed time	(sec)
Mass of char remaining	(gms)
Char gasified in the last time step	(gms)
Char gasified by CO_2 in the last time step	(gms)
Char gasified by H_2O in the last time step	(gms)
Specific gasification rates for CO_2 and H_2O calculated for last time step for largest particles	(gm/cm^2-sec)
Particle diameters	(cm)
Char mass distribution	(gms)

Nonequilibrium mole fractions - mole fractions
prior to equilibration

Equilibrium mole fractions

Temperature (^{o}K)

Iterations - the number of iterations required
to establish equilibrium conditions

Equilibrium parameter - the parameters Ψ or Ψ'
defined in the text

Equilibrium direction - a value of +1 indicates
the forward reaction of $H_2O + CO \rightleftarrows CO_2 + H_2$.
A value of -1 indicates the reverse reaction.

For calculations conducted assuming a coal size distribution of 100%-200 mesh, WTPCT(5) through WTPCT(7) were set to zero. To prevent division by zero during the calculations, the loop initiated at Statement #93 was performed only four times.

```
C
C
C      CHAR GASIFICATION CALCULATIONS
C   SPECIES= 1-H2O, 2-CO, 3-CO2, 4-H2, 5-N2, 6-C
C    CP AND HO ARE IN CAL/GM/K AND CAL/GM
C   FORWARD RKTN IS DEFINED AS    H2O + CO = H2 + CO2
C     1 ATM = 1.012E06 DYNE/CM-CM

      INTEGER RKTN
      REAL MW,MWAV,MWAVP,MC,MTOT,MCO,MCGAS,MP,NPART,NTOT
      REAL MCGAS1, MCGAS2
      DIMENSION X(6), XP(5), FAC1(6), FAC2(6)
      DIMENSION MW(6), HO(6), CP(6)
      DIMENSION D(7), WTPCT(7), PMC(7)
      DIMENSION NPART(7)

      DATA (CP(I),I=1,6)/.681,.309,.328,4.10,.307,.35/
      DATA (HO(I),I=1,6)/-3211.,-943.43,-2137.5,0.,0.,-1778.8/
      DATA(MW(I),I=1,6)/18.,28.,44.,2.,28.,12./
      DATA(WTPCT(I),I=1,7)/.1165,.1941,.2639,.2028,.1120,.0697,.041/
      DATA(D(I),I=1,7)/.0005,.0017,.0036,.0063,.0093,.0125,.0178/

      READ(5,1000) P, RHOP, NTOT
      READ(5,1001) MC, T
      READ(5,1002) X
      READ(5,1003) XP
      READ(5,1004) NTSTEP, NESTEP
1000  FORMAT(3E10.3)
1001  FORMAT(2E10.3)
1002  FORMAT(6F10.3)
1003  FORMAT(5F10.3)
1004  FORMAT(2I5)

      KFUEL=0
      MCO=MC
      Z11= .044 * MCO
      Z3= .01 * MCO
      Z12=1./3.
      TIME=0.
      MWAV=0.
      H=0.
      DO 10  I=1,7
      PMC(I) = MCO*WTPCT(I)
10    NPART(I)=PMC(I)*6./(RHOP*3.14*D(I)*D(I)*D(I))
      DO 100  I=1,6
100   MWAV= MWAV + (MW(I)*X(I))
      MTOT=MWAV * NTOT
      DO 105  I=1,6
       FAC1(I)=HO(I)*MW(I)/MWAV
      FAC2(I)= CP(I) * MW(I)/MWAV
105   H=H+(X(I)*FAC1(I))+((T-298.)*X(I)*FAC2(I))

      WRITE(6,2999)
      WRITE(6,3000) D
      WRITE(6,3001) WTPCT
      WRITE(6,3002) P, RHOP, NTOT
      WRITE(6,3003) T, MC
```

```
      WRITE(6,3004) X
      WRITE(6,3005) NPART
      WRITE(6,3006) PMC
      WRITE(6,3018)  MWAV
      WRITE(6,3007) H

C     START TIME STEP ITERATIONS

      DO 900  II=1,NTSTEP
      DTIME=.001
      IF (II .GT. 20) DTIME=.010
      IF (II .GT. 23) DTIME=.025
      TIME=TIME+DTIME
      MCGAS=0.
      MCGAS1=0.
      MCGAS2=0.
      MWAVP=(MTOT-MC)/(NTOT-(MC/12.))
      DIFF1=(2.42*1.012*(10.**6.)/P)*((T/1500.)**1.75)
      DIFF2=(4.25*1.012*(10.**6.)/P)*((T/1500.)**1.75)
      ALFA1=27.
      IF (T .LE. 2460.) GO TO 110
      ALFA1=2.511*(10.**9.)/EXP(88013./(T*1.986))
  110 CONTINUE
      ALFA2=4905./EXP(16315./(T*1.986))
      IF (T .LE. 2646.) GO TO 111
      ALFA2=3.698*(10.**12.)/EXP(123740./(T*1.986))
  111 CONTINUE
      RHOAVP=P*MWAVP*1.205/(T*(10.**8.))
      YCO2P=(44.*X(3))/(MWAVP*(1.-X(6)))
      YH2OP=(18.*X(1)) /(MWAVP*(1.-X(6)))
      DO 115 I=1,7
      Z1=(D(I)/(DIFF1*2.)) + (1./ALFA1)
      Z2=(D(I)/(DIFF2*2.)) + (1./ALFA2)
      QDPP1=12.*YCO2P*RHOAVP/(44.*Z1)
      QDPP2=12.*YH2OP*RHOAVP/(18.*Z2)
      PMCGS1 =3.14*D(I)*D(I)*DTIME*NPART(I)*QDPP1
      PMCGS2 =3.14*D(I)*D(I)*DTIME*NPART(I)*QDPP2
      PMCGAS=PMCGS1 + PMCGS2
      IF (PMCGAS .LE. PMC(I)) GO TO 113
      PMCGAS=PMC(I)
      PMCGS1=0.5 * PMCGAS
      PMCGS2=PMCGS1
  113 CONTINUE
      MCGAS= MCGAS + PMCGAS
      MCGAS1 = MCGAS1 + PMCGS1
      MCGAS2 = MCGAS2 + PMCGS2
      PMC(I)= PMC(I)-PMCGAS
  115 D(I)=(6.*PMC(I)/(3.14*RHOP*NPART(I)))**Z12
      MC=MC-MCGAS
      IF ( MC .LE. Z3 ) KFUEL=1
      X(6)=X(6)-(MCGAS/(12.*NTOT))
      X(4)=X(4)+(MCGAS2/(12.*NTOT))
      X(3)=X(3)-(MCGAS1/(12.*NTOT))
      X(2)=X(2)+(MCGAS2/(12.*NTOT))+(MCGAS1/(6.*NTOT))
      X(1)=X(1)-(MCGAS2/(12.*NTOT))
      Z4=1.-X(6)
```

```
      WRITE(6,3008) TIME, MC, MCEAS
      WRITE(6,3015) MCGAS1, MCGAS2
      WRITE(6,3014) QDPP1, QDPP2
      WRITE(6,3009) D
      WRITE(6,3010) PMC
      WRITE(6,3011) X
      DO 130  I=1,5
  130 XP(I)=X(I)/Z4

C     START EQUILIBRIUM ITERATIONS

      DO 300  JJ=1,NESTEP
      Z9=(1750./T)-1.515
      KP=10.**Z9

C   ASSUME FORWARD REACTION

      YA=1.-KP
      YB=((XP(3)+XP(4))/XP(1)) + (KP*(1.+(XP(2)/XP(1))))
      YC=(XP(3)*XP(4)/(XP(1)*XP(1))) - (KP*XP(2)/XP(1))
      YD=(YB*YB)-(4.*YA*YC)
      IF  (YD .LT. 0.) GO TO 210
      PSI1=(YB-SQRT(YD))/(-2.*YA)
      IF (PSI1 .GT. 1. .OR. PSI1 .LT. 0.) GO TO 201
      PSI=PSI1
      GO TO 205
  201 PSI2=(YB+SQRT(YD))/(-2.*YA)
      IF (PSI2 .GT. 1. .OR. PSI2 .LT. 0.) GO TO 210
      PSI=PSI2
  205 XP(3)=XP(3)+(PSI*XP(1))
      XP(4)=XP(4)+(PSI*XP(1))
      XP(2)=XP(2)-(PSI*XP(1))
      XP(1)=XP(1)-(PSI*XP(1))
      RKTN=1
      GO TO 215

C     CALCULATIONS FOR BACKWARD REACTION

  210 YA=1.-KP
      YB=-1.-(XP(3)/XP(4))-(KP*((XP(2)/XP(4))+(XP(1)/XP(4))))
      YC=(XP(3)/XP(4))-(KP*XP(1)*XP(2)/(XP(4)*XP(4)))
      YD=(YB*YB)-(4.*YA*YC)
      IF (YD .LT. 0.) GO TO 214
      PSI1=(YB-SQRT(YD))/(-2.*YA)
      IF (PSI1 .GT. 1. .OR. PSI1 .LT. 0.) GO TO 211
      PSI=PSI1
      GO TO 213
  211 PSI2=(YB+SQRT(YD))/(-2.*YA)
      IF ( PSI2 .GT. 1. .OR. PSI2 .LT. 0.) GO TO 214
      PSI=PSI2
  213 XP(1)=XP(1) + (PSI*XP(4))
      XP(2)=XP(2) + (PSI*XP(4))
      XP(3)=XP(3) - (PSI*XP(4))
      XP(4)=XP(4) - (PSI*XP(4))
      RKTN=-1
      GO TO 215
```

```
214   WRITE (6,2000)
      GO TO 950

215   CONTINUE

      DO 240  I=1,4
240   X(I)=XP(I)*Z4
      Z5=0.
      Z6=0.
      DO 250  I=1,6
      Z5=Z5+(X(I)*FAC1(I))
250   Z6=Z6+(X(I)*FAC2(I))
      TNEW=(H-Z5)/Z6
      TNEW= TNEW + 298.
      Z7=ABS(T-TNEW)
      IF (Z7 .LE. 5.) GO TO 350
      T=TNEW
      IF (JJ .EQ. NESTEP) WRITE(6,2001)
300   CONTINUE

350   CONTINUE
      WRITE(6,3012) X
      WRITE(6,3013) T, JJ, PSI, RKIN
      IF(KFUEL .EQ. 1) GO TO 950
      IF(II .EQ. NTSTEP ) WRITE(6,2002)

900   CONTINUE
950   CONTINUE

2000  FORMAT( ' NEGATIVE VALUE INSIDE SQUARE ROOT ')
2001  FORMAT( ' COMPLETED EQUIL STEPS')
2002  FORMAT( ' COMPLETED TIME STEPS ')
2999  FORMAT(/////,5X,'INITIAL CONDITIONS')
3000  FORMAT(///,5X,'INITIAL PARTICLE DIAMS. (CM)',/,5X,7E10.4)
3001  FORMAT(///,5X,'INITIAL WT. FRACTION DISTRIBUTION',/,5X,7E10.4)
3002  FORMAT(///,' PRESSURE=',E10.3,5X,'DENS=',E10.3,5X,'MOLES=',E10.3)
3003  FORMAT(///,' TEMP=',E10.4,5X,'GMS CARBON=',E10.4)
3004  FORMAT(///,' INITIAL MOLE FRACTIONS (H2O,CO,CO2,H2,N2,C) ',/,
     16F10.3)
3005  FORMAT(///,' PARTICLE NUMBER DISTRIB.',/,7E10.4)
3006  FORMAT(///,' CARBON MASS DISTRIB.',/,7E10.4)
3007  FORMAT(///,' INITIAL ENTHALPY (CAL/GM)=',E10.4,////////)
3008  FORMAT(////////,' TIME(SEC)=',E10.3,5X,'MASS CARBON=',E10.3,5X,
     1'CARBON GASIFIED=',E10.3)
3009  FORMAT(///,' PARTICLE DIAMS',/,7E10.4)
3010  FORMAT(///,' CARBON MASS DISTRIBUTION',/,7E10.4)
3011  FORMAT(///,' NONEQUIL. MOLE FRACTIONS',/,6E10.4)
3012  FORMAT(///,' EQUIL. MOLE FRACTIONS',/,6E10.4)
3013  FORMAT(///,' TEMP=',E10.4,5X,'ITERATIONS=',I5,5X,'EQUIL PARAM=',
     1E10.4,5X,'EQUIL DIRECTION',I5)
3014  FORMAT(///,' GASIF. RATE BY CO2 AND H2O (GM/CM-CM-SEC)',/,2E10.4)
3015  FORMAT(///,' GASIF. BY CO2 (GM)=',E10.4,5X,'GASIF. BY H2O=',E10.4)
3018  FORMAT(///,' AVG MOLECULAR WT=',E10.4)
      CALL EXIT
      END
```

INITIAL CONDITIONS

INITIAL PARTICLE DIAMS. (CM)
.5000-03 .1700-02 .3600-02 .6300-02 .9300-02 .1250-01 .1780-01

INITIAL WT. FRACTION DISTRIBUTION
.1165+00 .1941+00 .2639+00 .2028+00 .1120+00 .6970-01 .4100-01

PRESSURE= .607+07 DENS= .140+01 MOLES= .382+02

TEMP= .2722+04 GMS CARBON= .6708+02

INITIAL MOLE FRACTIONS (H2O,CO,CO2,H2,N2,C)
.122 .100 .065 .028 .539 .146

PARTICLE NUMBER DISTRIB.
.8533+11 .3617+10 .5179+09 .7426+08 .1275+08 .3267+07 .6656+06

CARBON MASS DISTRIB.
.7615+01 .1302+02 .1770+02 .1360+02 .7513+01 .4675+01 .2750+01

AVG MOLECULAR WT= .2476+02

INITIAL ENTHALPY (CAL/GM)= .9482+02

```
TIME(SEC)=    .100-02      MASS CARBON=    .642+02      CARBON GASIFIED=    .286+01

GASIF. BY CO2 (GM)=  .6116+00      GASIF. BY H2O=  .2245+01

GASIF. RATE BY CO2 AND H2O (GM/CM-CM-SEC)
 .1970-02  .6788-02

PARTICLE DIAMS
 .4638-03  .1669-02  .3574-02  .6278-02  .9282-02  .1248-01  .1779-01

CARBON MASS DISTRIBUTION
 .6237+01  .1233+02  .1732+02  .1346+02  .7469+01  .4656+01  .2744+01

NONEQUIL. MOLE FRACTIONS
 .1171+00  .1076+00  .6366-01  .3290-01  .5390+00  .1398+00

EQUIL. MOLE FRACTIONS
 .1200+00  .1105+00  .6074-01  .2998-01  .5390+00  .1398+00

TEMP=  .2681+04      ITERATIONS=    2      EQUIL PARAM=  .2800-02      EQUIL DIRECTION    1




TIME(SEC)=    .200-02      MASS CARBON=    .623+02      CARBON GASIFIED=    .191+01

GASIF. BY CO2 (GM)=  .4215+00      GASIF. BY H2O=  .1491+01

GASIF. RATE BY CO2 AND H2O (GM/CM-CM-SEC)
 .1652-02  .5705-02
```

References

1. Seikel, G. R.; and Harris, L. P.: A Summary of the ECAS MHD Power Plant Results. NASA TM X-73491, 1976.
2. TRW 25 MW_t Staged MHD Coal Combustor Conceptual Design Study. TID-27145, Energy Research and Development Adm., 1976.
3. MHD Combustor Design Study, TID-27144, Energy Research and Development Adm., 1976.
4. Golovina, E. S.; and Khaustovich, G. P.: Combustion of Carbon in Carbon Dioxide and Oxygen at Temperatures up to 3000° K. Eighth Symposium (Int.) on Combustion, The Combustion Institute, 1962, pp. 784-792.
5. Khitrin, L. N.; and Golovina, E. S.: Interaction Between Graphite and Various Chemically Active Gases at High Temperatures. High Temperature Technology, Butterworth and Co., Ltd. (London), 1963, pp. 485-496.
6. Field, M. A.; et al.: Combustion of Pulverized Coal. British Coal Utilization Research Assoc., (Leatherhead, Surrey), 1967.
7. Kobayashi, H.; Howard, J. B.; and Sarofin, A. F.: Coal Devolatilization at High Temperatures. Sixteenth Symposium (International) on Combustion, The Combustion Institute, 1977, pp. 411-425.
8. Gordon, S.; and McBride, B. J.: Computer Program for Calculation of Complex Chemical Equilibrium Compositions, Rocket Performance, Incident and Reflected Shocks, and Chapman-Jouguet Detonations. NASA SP-273, 1976, Revised.

9. Kanury, A. M.: Introduction to Combustion Phenomena: (For Fire, Incineration, Pollution, and Energy Applications). Gordon and Breach Science Publishers Inc., 1975.

10. Engineering Test Facility Conceptual Design. FE-2614, Parts 1 and 2, Dept. of Energy, 1978.

TABLE 1
PULVERIZED COAL SIZE DISTRIBUTIONS

70% minus 200 mesh							
Size Range (μm)	0-10	10-25	25-50	50-80	80-110	110-150	150
Characteristic Diameter (μm)	5	17	36	63	93	125	178
Mass Fraction	0.116	0.194	0.264	0.203	0.142	0.070	.011

100% minus 200 mesh				
Size Range (μm)	0-10	10-25	25-50	50-80
Characteristic Diameter (μm)	5	17	36	63
Mass Fraction	0.150	0.250	0.339	0.261

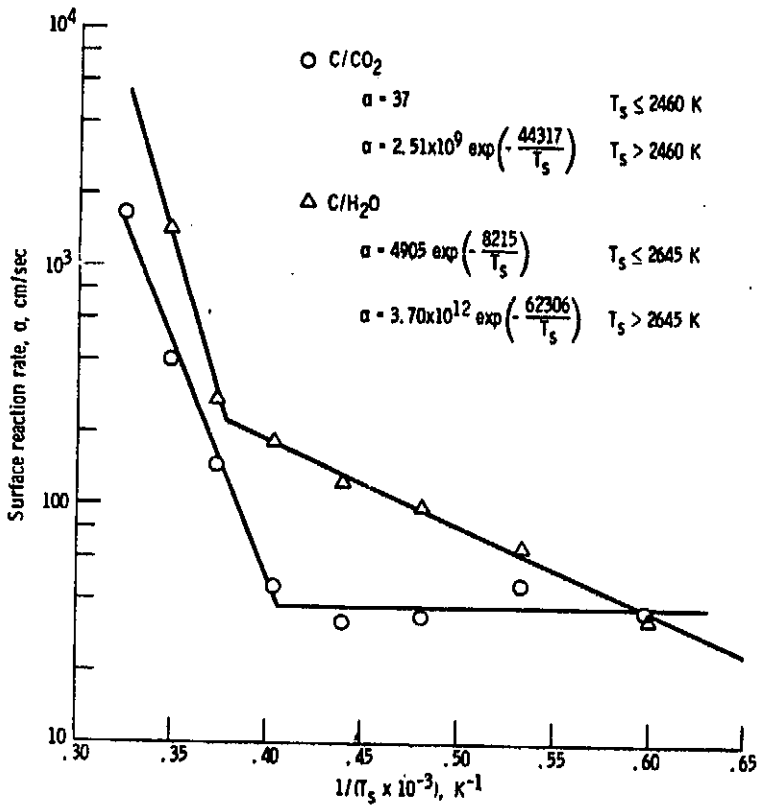

Figure 1. - Surface reaction rates of char with CO_2 and H_2O (refs. 4 and 5).

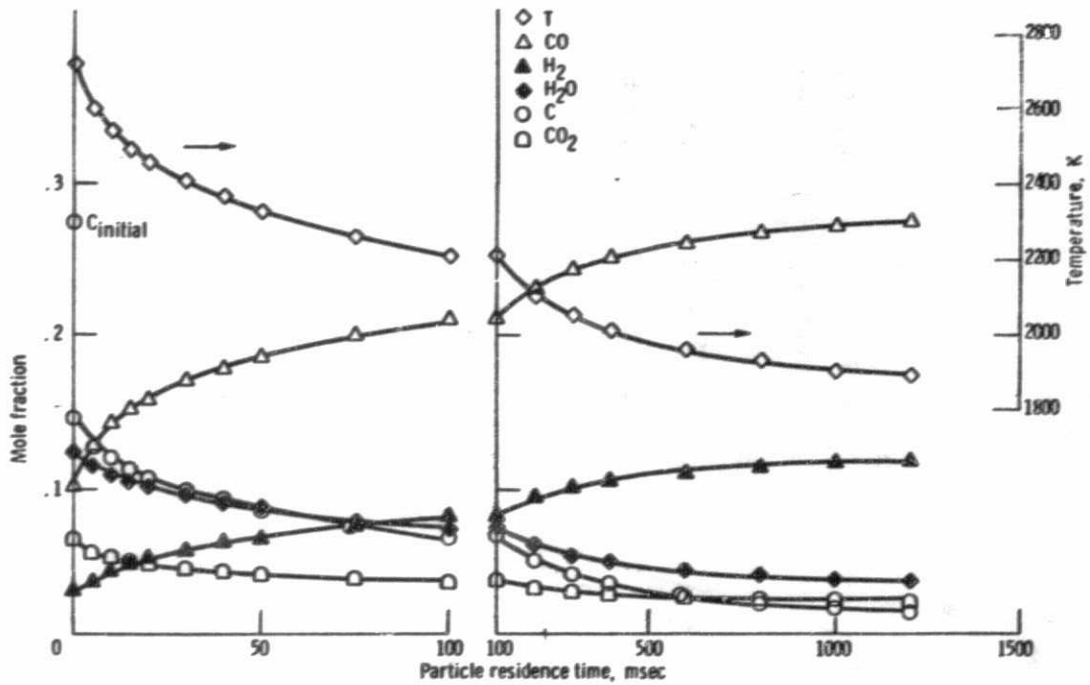

Figure 2. - Base case gasifier performance. 70 percent -200 mesh; ϕ_1 = 2.50; ξ_1 = 1.50; 10 percent heat loss; 100 percent moisture.

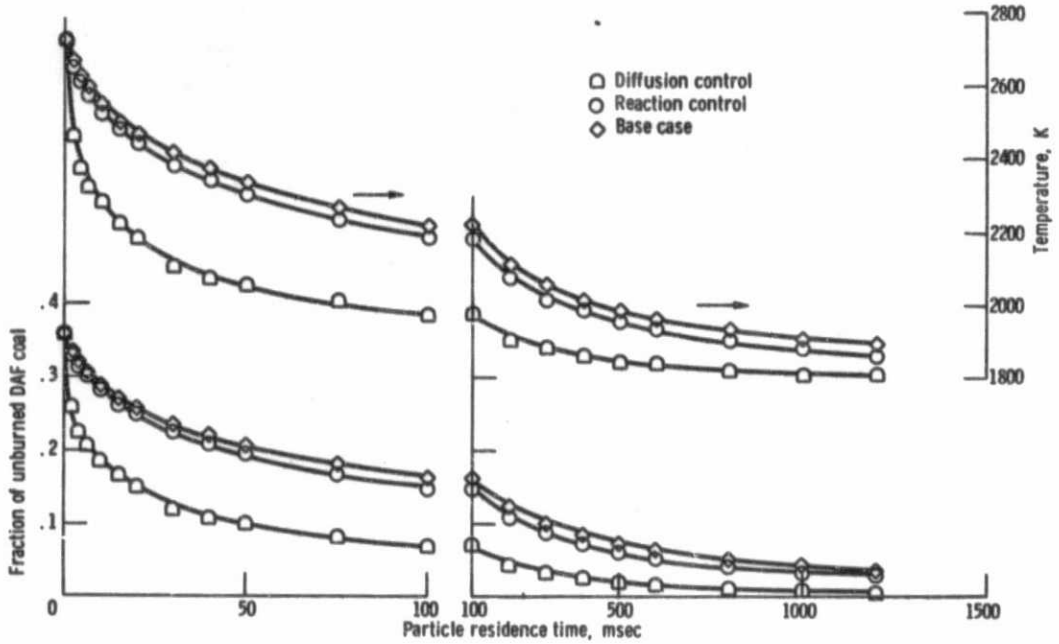

Figure 3. - Effects of surface reaction rates and diffusion rates on gasifier performance. 70 percent -200 mesh; φ_1 = 2.50; ξ = 1.50; 10 percent heat loss; 10 percent moisture.

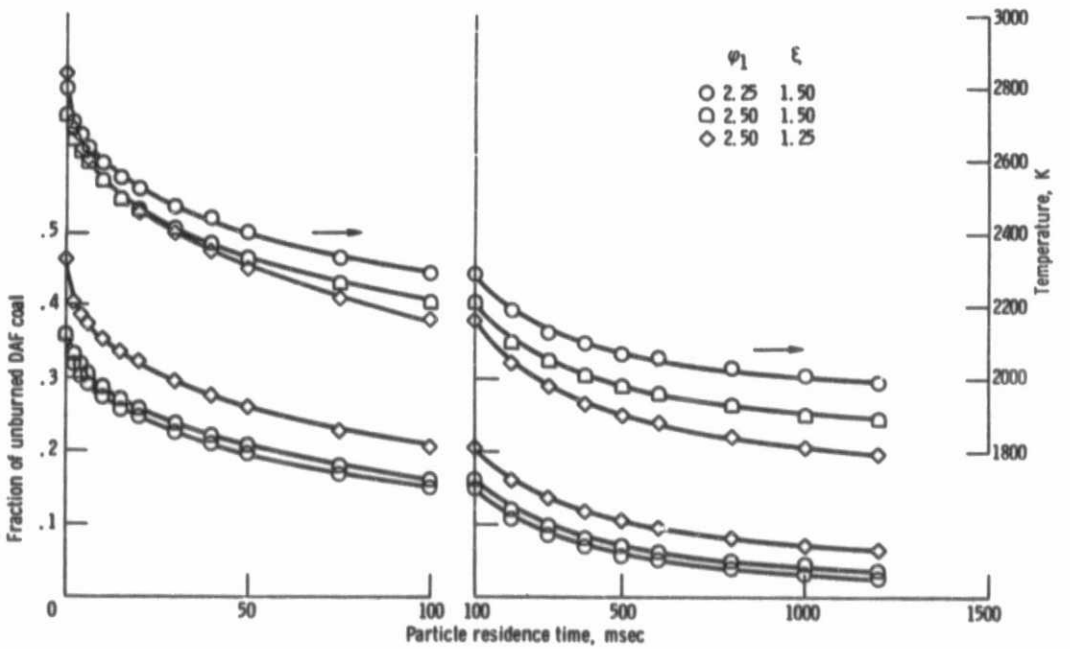

Figure 4. - Effect of equivalence ratio and degree of devolatilization on gasifier performance. 70 percent -200 mesh; 10 percent heat loss; 10 percent moisture.

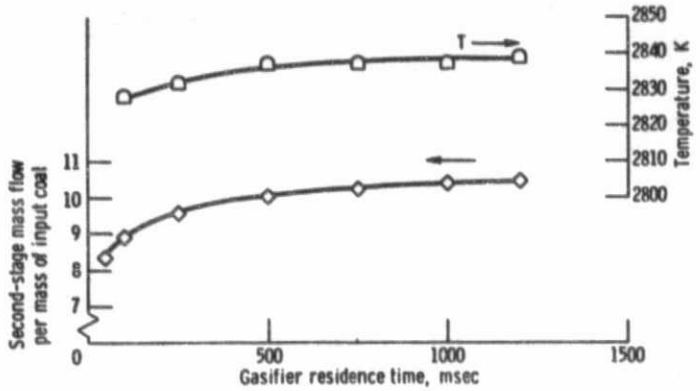

Figure 5. - Effect of gasifier residence time on second-stage performance. $\varphi_1 = 2.50$; $\xi = 1.50$; 70 percent -200 mesh; 10 percent heat loss; 10 percent moisture.

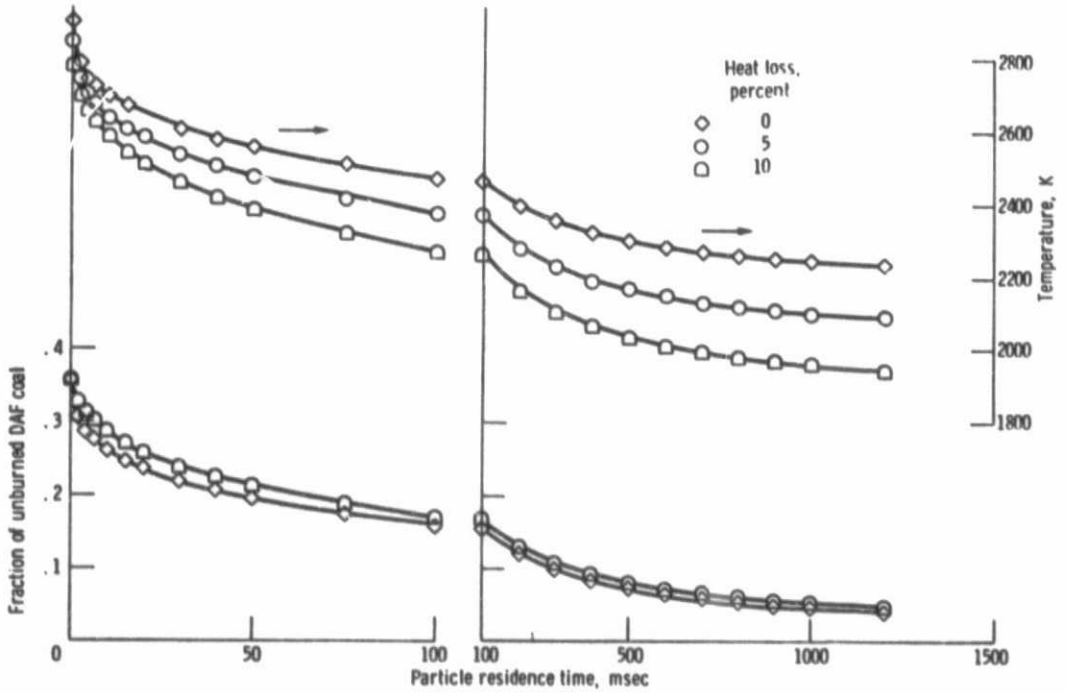

Figure 6. - Effect of combustor heat loss on gasifier performance. 70 percent -200 mesh; $\varphi_1 = 2.50$; $\xi = 1.50$; moisture = 5 percent.

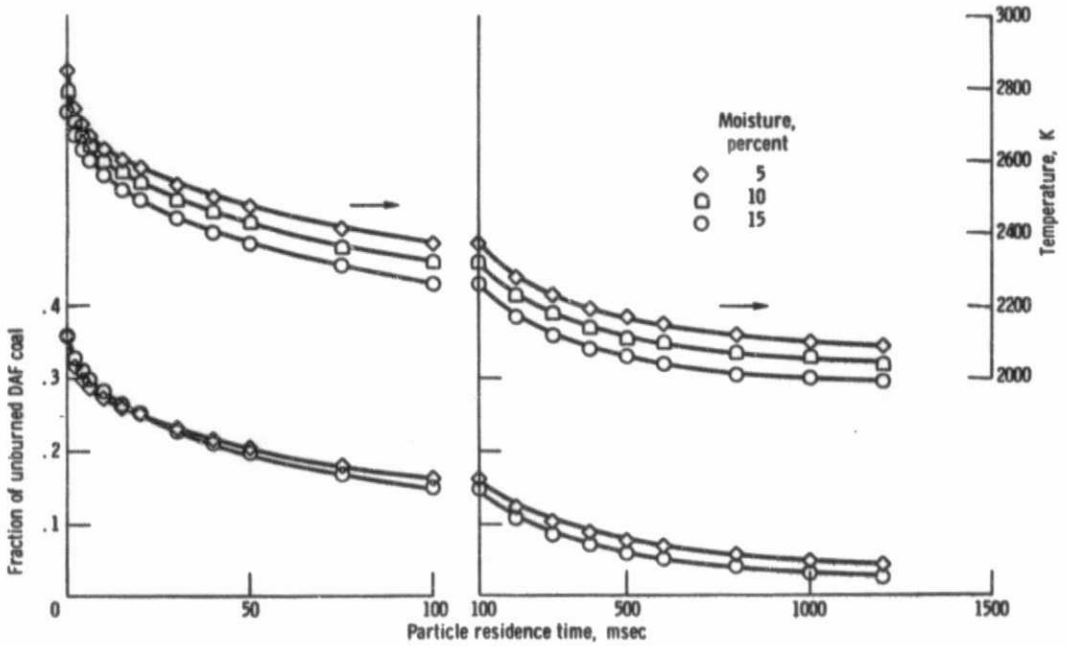

Figure 7. - Effect of coal moisture on gasifier performance. 70 percent -200 mesh; $\varphi_1 = 2.50$; $\xi = 1.50$; 5 percent heat loss.

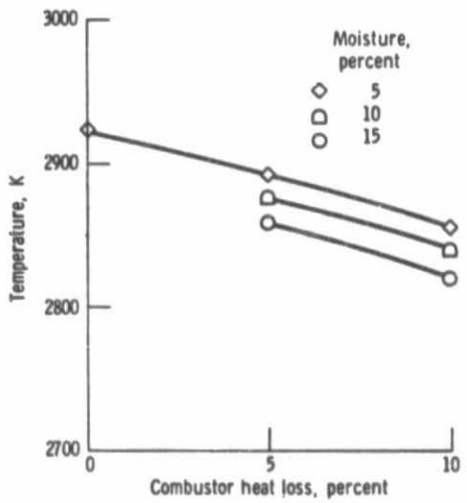

Figure 8. - Effect of combustor heat loss and coal moisture on second-stage combustor exit temperature. $\tau \geq 500$ msec; 70 percent -200 mesh; $\varphi_1 = 2.5$; $\xi = 1.5$.

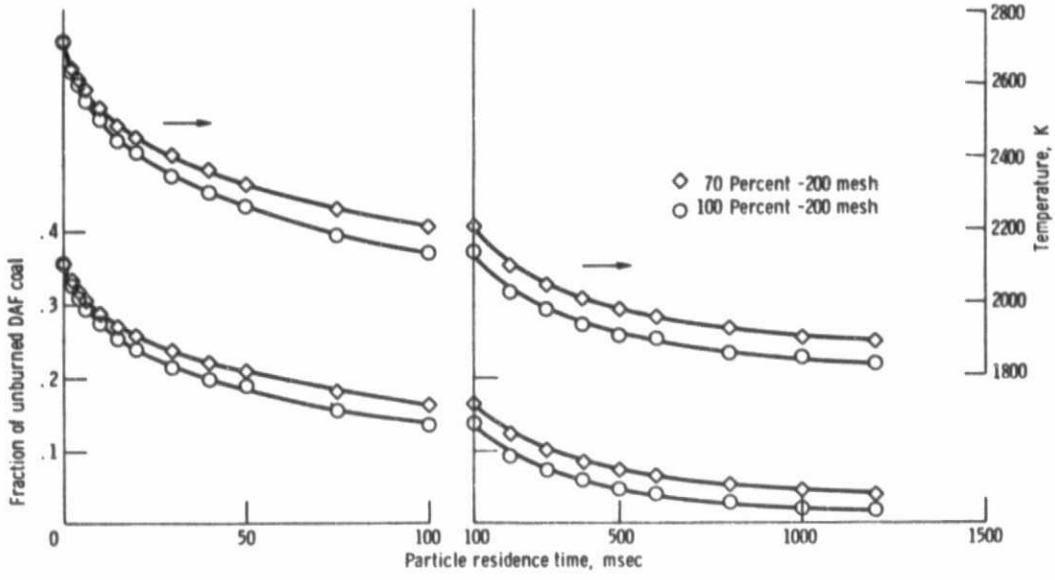

Figure 9. - Effect of coal size distribution on gasifier performance. $\varphi_1 = 2.50$; $\xi = 1.50$; 10 percent heat loss; 10 percent moisture.

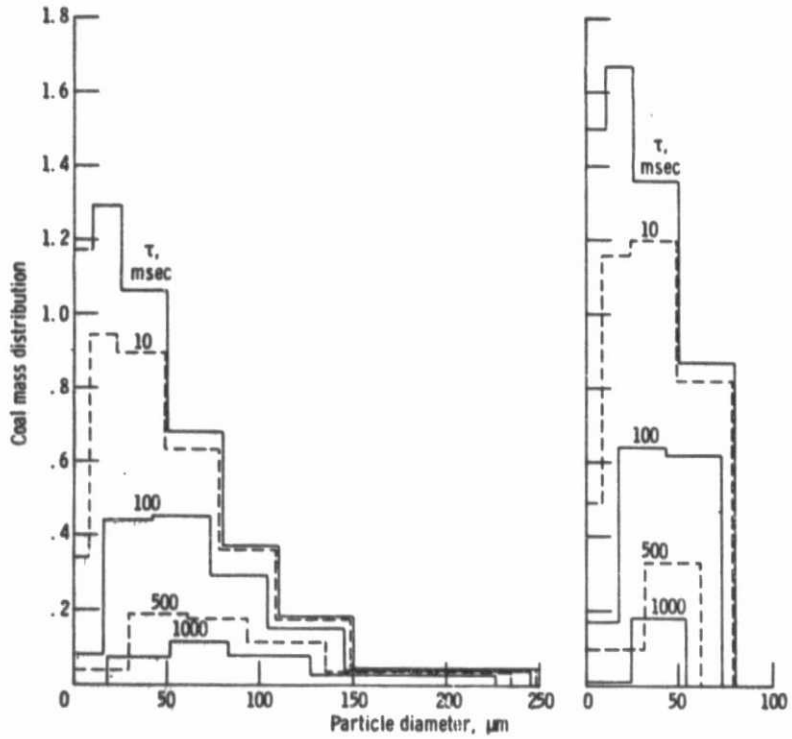

Figure 10. - Variation of coal mass distribution with residence time. φ_1 = 2.50; ξ = 1.50; 10 percent heat loss; 10 percent moisture.

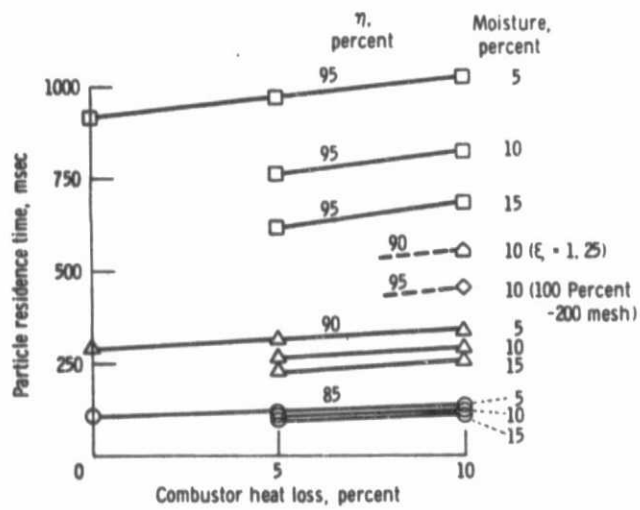

Figure 11. - Summary of gasifier performance predictions. φ_1 = 2.50; ξ = 1.50; 70 percent -200 mesh.